On-board lossless compression of Solar corona images

Marco Ricci, Enrico Magli

***Abstract*—The compression algorithm developed for METIS arises from the standard CCSDS 123.0-r-1 [?], a lossless data compressor suitable for multispectral and hyperspectral imagers and sounders. This paper presents an extension of the standard to handle lossless compression specifically tailored to solar corona images.**

The main contributions of this paper are the following: the adaptation to the radial geometry of solar corona images through a remapping process called "radialization" and the ability to exploit three-dimensional image compression of the standard through the compression of a multi-temporal data cube composed by successive acquisitions.

The development of the algorithm took care of many aspects based on the geometry and the nature of the expected acquisitions; this adaptation process leads to a significant increase in compression performance through routines resulting very light from a computational point of view, which is a key aspect for on-board applications.

I. Introduction

METIS, the Multi Element Telescope for Imaging and Spectroscopy, has been selected as coronagraph for the payload of the Solar Orbiter mission, aiming at a great number of scientific goals, such as determining properties and dynamic of plasma, fields and particles in the near-Sun heliosphere, identifying links between Sun's surface activities and evolution of the solar corona, observing and characterizing the Sun's polar regions and equatorial corona from high latitudes. In particular, the coronagraph, reaching a minimum distance from the Sun of 0,28 AU, will allow full imaging of the extended corona, in UV and visible light spectra. As it is for most nowadays imaging sensors, a significant amount of data is generated, making image compression essential to reduce the data volume before transmitting to the ground segment. The proposed algorithm provides a low-complexity predictive-based compression scheme, derived from an international standard but presenting several innovative aspects, both in the kind of compression approach and in some ad-hoc routines enhancing its performance.

The development of the compression algorithm has been based on the following requirements:

1) the computational resources available on-board are limited, so a low degree of complexity is mandatory;
2) the need of a high level of compression requires an ad-hoc algorithm development;

A preliminary analysis has been performed [**?**] employing the JPEG-LS [**?**], JPEG-2000 [**?**] and CCSDS image data compression standard [**?**], showing that the predictive approach is best suited to accomodate low complexity and high compression efficiency. As a consequence, in this paper we propose an extension of a recent standard by the Consultative Committee for Space Data System, named CCSDS-123 [**?**]; it is natively a predictive lossless data compression algorithm applicable to three-dimensional image data from payload instruments, such as multispectral and hyperspectral imagers.

In this paper we describe the lossless extensions to CCSDS-123. The full algorithm, which also supports different modalities of lossy compression, will be described in a forthcoming paper.

II. Review of CCSDS-123 standard

The standard follows the typical scheme of lossless compression, employing a prediction-based approach; this aspect provides a further advantage: as opposed to the transform-based scheme, it guarantees a low computational complexity that is a key constraint to be suitable for on-board applications. The input to the compressor is a three-dimensional array of integer sample values; the variable-length compressed output is an encoded bitstream from which the input image can be exactly recovered. The compression process is simply composed by two functional parts: a predictor followed by an encoder. The prediction of the sample $s_{x,y,z}$ consists in the calculation of a predicted value $\hat{s}_{x,y,z}$ from which the mapped residual $\delta_{x,y,z}$ can be derived. The procedure to compute the predicted value involves a three-dimensional neighborhood: first, the predictor computes a local average of neighboring sample values; a weighted sum of neighboring samples from the current and a user-defined number of previous bands is then calculated, and finally the predicted value can be obtained by subtracting from this weighted sum, the previously computed local average. One of the main features of this standard is the capability of the predictor to adapt to the local statistics, using the prediction error of every pixel to enhance the computation of the following predicted values, through a weight update. The mapped residual $\delta_{x,y,z}$, of every pixel, a non-negative integer value, is encoded using a variable-length binary codeword composing the body of the compressed file. The variable-length codes are adaptively selected based on statistics that are updated after each sample is encoded; separate statistics are kept for each spectral band and the compressed image size does not depend on the order in which residuals are encoded. Upon the body of the compressed image, there is the header holding all the information of the image essential for decoding and to reconstruct exactly the input image.

While the algorithm has state-of-the-art performance for lossless compression, it needs to be tailored to all other requirements for solar corona images,
Consequently, the standard has been adapted in order to comply with all the requirements and to provide top performance for solar corona images; this has resulted in an algorithm design with the following innovative features:

- compression of multitemporal solar corona image stacks;
- image reordering through a "radialization" process, in order to exploit the peculiar image geometry;
- standard binning or radial binning on circular or rectangular coronae image areas respectively;

III. Proposed compression algorithm

This section will present the modifications to the standard to make it properly work with the sensor output images. First, the idea of keeping the three-dimensional compression ability of the standard but adapted ad-hoc for the mission purpose is explained, and further, the pre-processing routine to adapt to the image geometry is presented.

A. Multitemporal compression

While the CCSDS-123 standard can compress three-dimensional images, solar corona images are not characterized by multiple spectral channels. On the other hand, onboard a coronagraph, several images are usually acquired in temporal sequence, therefore the multidimensional compression capability has been kept but adapted to the mission purpose. In particular we exploit the similarity of time-consecutive acquisitions, switching the third dimension from wavelength to time; the gain in terms of compression performance is significant with respect to the individual compression of each image.

B. Radialization

One of the most innovative parts of the compression algorithm consists in a pre-processing routine developed to exploit the radial symmetry of solar corona.
It is an algorithm named "radialization", which consists in rearranging the positions of the image pixels switching from a cartesian coordinates system to a polar one, in which the two dimensions are the distance of each pixel from the center of the image, and the angle with respect to a reference.
Essentially, the radialization process scans the image from the center towards its boundary, in circles of increasing radius. In this way, pixels that are expected to have similar values are adjacent in the radialized image, minimizing discontinuities encountered along the scanning pattern. This provides two benefits. First, since correlation is maximized in the radialized image, compression is expected to be more efficient. Second, the radialized image lends itself well to defining region of interest in the form of circular coronae, which is a much more natural geometry than rectangular images for a coronagraph.
A pseudo code of it is presented in algorithm **??**. The compression process is applied to the radialized image. The decoded radialized image undergoes inverse permutation in order to restore the original image geometry.
The user has to specify a circular coronal-shaped masking of the input image (an example is shown in figure **??**b), by defining an internal and and external radius, whose minimum value is zero, and whose maximum value corresponds to the radius of the biggest inscribed circle within the input image.

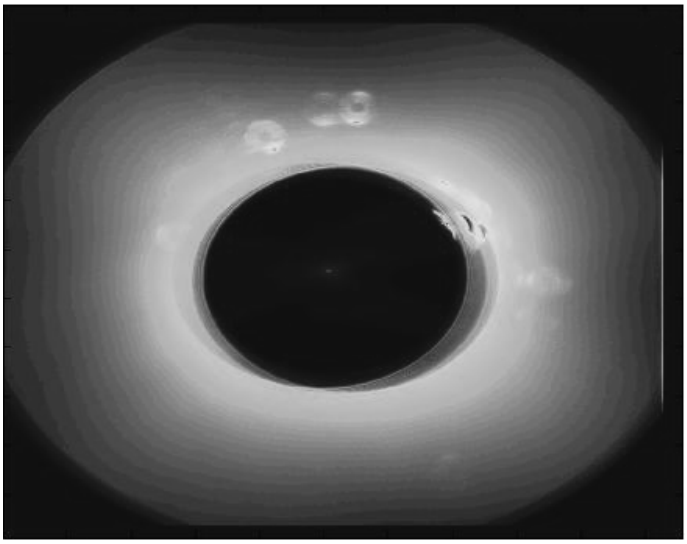

Fig. 1: Example of a solar corona acquisition

The values are first written in a matrix structure in which the only discriminating factor is the distance from the center, corresponding to the rows of the radialized image; the angles, instead are temporarily saved in another structure; all the angles of pixel values with the same distance to the image center, i.e. belonging to the same radialized image rows, are then ordered by increasing value. The sorting is kept and applied to the structure storing the actual values, in such a way that every radialized image row includes pixels in the original domain with the same distance to the center and sorted by increasing angles, following a circular-shaped path.

In this way, the obtained output is the radialized image, as shown in figure **??** and figure **??** for variable radialization radii.

The most significant and original aspect of radialization is that no interpolation among pixels, which is typical when changing a reference system, is performed; actually it can be seen as a permutation of the original pixels, according to the new geometry; therefore the lossless property of the compression algorithm can be exactly preserved, since pixel values stays unaltered through the radialization process.
Further, another advantage lies in the need of executing the whole algorithm just once at initialization, since the mapping between the input image and the radialized image only depends on the image size and not on the pixel values.

Algorithm 1 Radialization algorithm

[M,N] = size(input_image)
for $i = 0; i < N; i++$ **do**
  for $j = 0; j < M; j++$ **do**
    $dist = round(\sqrt{(i-x_c)^2 + (j-y_c)^2})$
    if $R \leq dist \leq r$ **then**
      radial(dist,pos(dist)) = input_image(i,j)
      angles(dist,pos(dist)) =
      $= 2 \cdot \arctan \frac{(j-y_c)}{\sqrt{(i-x_c)^2+(j-y_c)^2}+i-x_c}$
    end if
    pos(dist) ++;
  end for
end for
ordered_angles(i,j) = **sort**(angles,$rows$)
for $i = 0; i < N; i++$ **do**
  for $j = 0; j < M; j++$ **do**
    K $\leftarrow$ ordered_angles(I,k) == angles(I,j)
    ordered_radial(i,j) = radial(i,ordered_angles(i,j))
  end for
end for
for $i = 0; i < N; i++$ **do**
  for $j = 0; j < M; j++$ **do**
    shift ordered_radial(i,j) $\rightarrow$ ordered_radial(i,N-pos(i)+j)
  end for
end for

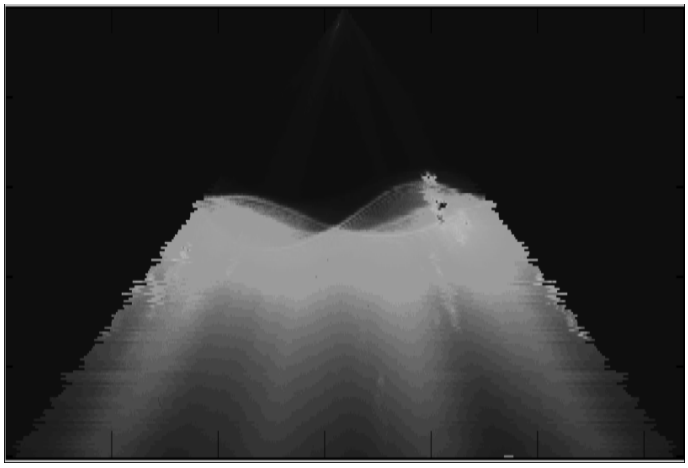

Fig. 2: Radialized image with default settings, null internal radius and external radius equal to the half of input image dimension

IV. Performance assessment

This section will present the advantages of the presented compression algorithm, showing how a three-dimensional image compression is much more efficient compared to the two-dimensional case, and the efficiency of radialization.
The set of images used to test the algorithm comes from two coronagraphs belonging to the mission STEREO (Solar TErrestrial RElation Observatory), consisting in the launch of two nearly identical spacecrafts, one ahead of Earth in its orbit, the other trailing behind; it allowed the first-ever stereoscopic imaging of the Sun and its related phenomena.

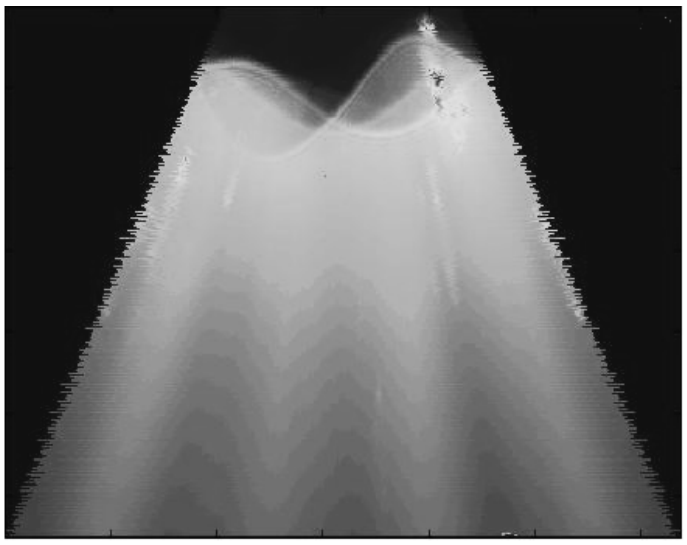

Fig. 3: Radialized image with non-null internal radius

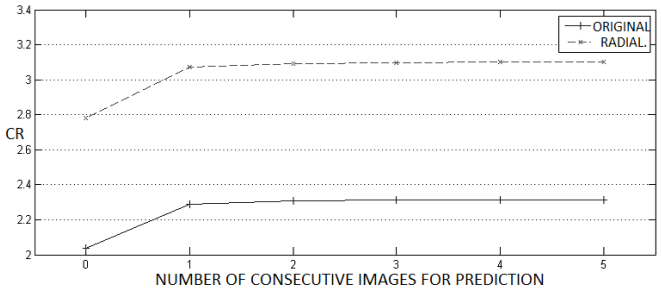

Fig. 4: Compression performance varying the number of consecutive images to be used for prediction (coronograph STEREO-A)

An occulter conceals the Sun center, to highlight the real section of interest which is the Solar corona, in particular the area closest to the Sun, where Coronal Mass Ejections (CMEs) take place and are visible. The samples dynamic range is 16 bits.

Simulations have been run in order to prove that multi-temporal compression is advantageous if compared to a two-

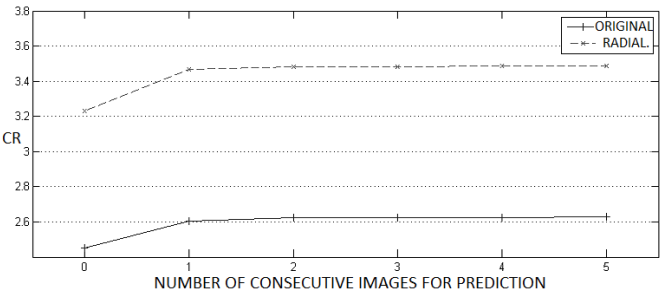

Fig. 5: Compression performance varying the number of consecutive images to be used for prediction (coronograph STEREO-B)

dimensional image compression; this has been verified for both standard and radialized three-dimensional acquisitions, by feeding the compressor with a data cube of time-consecutive images, and tuning the parameter that drives the number of acquisitions to be used in the prediction process; if this value is set to zero, it would mean compressing every image singularly, by employing a 2D neighborhood in the prediction loop. As soon as it increases, consequently the values of the compression ratio (CR) increase consistently, as shown in figures **??** and **??**.

The CR here considered is always computed with respect to the original image size; considering it, the shown performance already gives the idea of how much compressing radialized acquisitions outperforms the compression of standard images. In particular, radialization provides an increase of compression ratio from about $2.3 : 1$ to about $3.1 : 1$, which is very significant. Moreover, the compression of a set of multitemporal images, as opposed to a single image, increases the compression ratio by about 10%. The combination of these two elements allows to improve the compression ratio from about $2 : 1$ to about $3.1 : 1$ for STEREO-A, which corresponds to about 2.5 bits per pixel.

V. Conclusions

The developed compression algorithm provides an innovative design in several aspects; it is tailored to the expected acquisitions from METIS sensors, but the radialization routine can be applied on a large variety of images with a similar geometry.
Further, a key aspect is the derivation from a state-of-the-art performing standard, such as the CCSDS-123.

References

[1] *Lossless Multispectral & Hyperspectral Image Compression CCSDS 123.0-R-1*, ser. Red Book (draft). CCSDS, May 2011, available at `http://public.ccsds.org/sites/cwe/rids/Lists/CCSDS201230R1/Attachments/123x0r1.pdf` (June 2013).

[2] Bemporad, G. Nicolini, B. Zhao, E. Magli, *"Performance assessment of lossy compression algorithms for application to METIS solar probe"*, in 2012 Onboard Payload Data Compression Workshop (OBPDC), Barcelona (Spain), Oct. 2012. pp. 1-8

[3] Pennebaker, W. B. & Mitchell, J. L. (1993). *"JPEG Still Image Data Compression Standard"*. New York: Van Nostrand Reinhold. ISBN 0-442-01272-1.

[4] Majid Rabbani*, Rajan Joshi, *"An overview of the JPEG2000 still image compression standard"*, in Signal Processing: Image Communication 17 (2002) 3-48

[5] Recommended Standard, Issue 1, blue book *"ccsds recommended standard for image data compression"*